



# Brain volumetric changes in patients with spinocerebellar ataxia type-2

Baris Genc<sup>a,\*</sup>, Sedat Sen<sup>b</sup>, Kerim Aslan<sup>a</sup>

<sup>a</sup>Ondokuz Mayıs University, Faculty of Medicine, Department of Radiology, Samsun, Türkiye

<sup>b</sup>Ondokuz Mayıs University, Faculty of Medicine, Department of Neurology, Samsun, Türkiye

## ARTICLE INFO

### Keywords:

SCA2

Voxel-based morphometry  
Surface-based morphometry  
Cortical thickness  
Subthalamic nucleus

Received: May 30, 2024

Accepted: Aug 22, 2024

Available Online: 28.08.2024

DOI:

[10.5455/annalsmedres.2024.03.062](https://doi.org/10.5455/annalsmedres.2024.03.062)

## Abstract

**Aim:** Spinocerebellar ataxia type 2 (SCA2) is a trinucleotide repeat disorder characterized by mutations in the ataxin-2 gene. Although the primary symptoms of this disease are related to cerebellar involvement, such as ataxia and dysarthria, cognitive disorders associated with supratentorial involvement, depression, and extrapyramidal symptoms are also common. The aim of this study was to investigate volumetric changes in patients with SCA2.

**Materials and Methods:** Nine SCA2 patients and sixteen age and gender-matched healthy controls were included in the study. Voxel-based morphometry (VBM) was used to explore changes in whole brain gray and white matter, while surface-based morphometry (SBM) was employed to investigate changes in cortical thickness (CT), local gyrification index (LGI), sulcal depth (SD), and fractal dimension (FD). Deep learning methods were utilized for the automatic segmentation of subcortical gray matter structures and extrapyramidal system structures. Comparisons between groups were made using GLM, T-Test, and Mann-Whitney U test.

**Results:** VBM results showed widespread gray matter loss in the cerebellum and widespread white matter loss in the brain stem (Cluster size: 25918 voxels for gray matter, 24557 voxels for white matter). SBM findings indicated a decrease in cortical thickness (Cluster size: 19276 vertices for left hemisphere; 17276 vertices for right hemisphere), more pronounced in the supratentorial frontoparietal region, while FD, LGI, and SD did not differ between groups. Volume loss was observed in the subthalamic nucleus, globus pallidus internus and externus, and red nucleus in SCA2 patients.

**Conclusion:** SCA2 patients exhibit white and gray matter volume loss in the infratentorial region. Additionally, they show a decrease in frontoparietal cortical thickness, while FD, LGI, and SD do not show any changes. Moreover, atrophy is also observed in the extrapyramidal system structures.



Copyright © 2024 The author(s) - Available online at [www.annalsmedres.org](http://www.annalsmedres.org). This is an Open Access article distributed under the terms of Creative Commons Attribution-NonCommercial-NoDerivatives 4.0 International License.

## Introduction

Spinocerebellar ataxia type 2 (SCA2) is the second most common form of spinocerebellar ataxia, following SCA type 3 [1]. It is an autosomal dominant trinucleotide repeat disorder caused by mutations in the ataxin-2 (ATXN2) gene. Mutations in this gene primarily affect the Purkinje fibers, the inferior olive, and the pontine nucleus [2]. The main symptom in SCA2, due to the cerebellum being affected, encompasses ataxic gait, dysarthria, and dysmetria related to cerebellar involvement. However, SCA2 also encompasses cognitive impairment, depression, and extrapyramidal symptoms, indicating that the disease's impact is not confined to posterior fossa structures

but may also affect supratentorial regions [3].

Voxel-based morphometry (VBM) studies investigating gray matter changes in SCA2 patients have demonstrated widespread involvement in the cerebellum and brainstem [4, 5, 6, 7], yet only a few have demonstrated limited supratentorial involvement [8, 9], conflicting with other VBM studies which did not show such involvement. Surface-based morphometry (SBM) is an increasingly popular morphometric method in recent years, enabling the detection of morphometric parameters such as cortical thickness (CT), sulcal depth (SD), fractal dimension (FD), and local gyrification index (LGI), which are not discernible through VBM [10]. A few SBM studies on SCA2 patients have revealed reductions in supratentorial CT [11], and in both supratentorial and infratentorial cortical complexity [12], which were not detectable through VBM. However, to

\*Corresponding author:

Email address: [barisgenc12@gmail.com](mailto:barisgenc12@gmail.com) (Baris Genc)

our knowledge, there are no studies exploring other SBM parameters such as sulcal depth and local gyrification index. The pattern of atrophy in neurodegenerative diseases varies, with some diseases showing pronounced sulcal depth while others exhibit more prominent gray matter atrophy [13, 14]. There is no known study that concurrently utilizes VBM and SBM for a comprehensive volumetric assessment to investigate the dominant atrophic pattern in SCA2, a neurodegenerative disease.

Although extrapyramidal involvement in SCA2 patients and its supporting pathology, including atrophy and gliosis of the substantia nigra, subthalamic nucleus, and globus pallidus, have been documented in pathology series [15], no study to our knowledge has demonstrated this in-vivo using MRI. However, a recent deep learning algorithm can segment extrapyramidal structures such as the subthalamic nucleus, internal globus pallidus (Gpi), and substantia nigra from volumetric T1 images with high accuracy [16].

The aim of this study is to employ a broad volumetric spectrum to elucidate the pathophysiology and neurodegenerative underpinnings in SCA2 patients by detecting infratentorial and supratentorial changes using VBM and SBM methods, and to identify volumetric changes in subcortical gray matter structures and extrapyramidal structures utilizing deep learning algorithms.

## Materials and Methods

This observational study utilized clinical and MRI images licensed under the Creative Commons Attribution 4.0 International (CC-BY 4.0) from a Public Dataset (<https://openneuro.org/datasets/ds001378/versions/00003>). Given that the public dataset had already received ethical approval from the Careggi University Hospital of Florence, Italy [17]. Ethical approval for the study was obtained (Ondokuz Mayıs University Clinical Research and Ethics Committee, Decision no: 2024/171). The findings are presented in accordance with the Strengthening the Reporting of Observational Studies in Epidemiology (STROBE) guidelines [18].

### Subjects

All patients and healthy volunteers in the 'ds001378' dataset were included in the study. Since all patients and the control group in the dataset were used, a power analysis was not conducted to determine the sample size. Nine SCA2 patients, genetically confirmed and over the age of 18, who were able to walk without the assistance of a caregiver, without any neurological comorbidities or MRI contraindications, and sixteen healthy volunteers matched for age and gender were included in the study.

### MRI

MRI images were obtained using a 1.5 Tesla device (Intera, Philips Healthcare, Best, Netherlands) with a 6-channel head coil. 3D T1 images were acquired using a turbo gradient echo sequence (160 contiguous sagittal slices with an in-plane voxel resolution of  $1 \times 1 \times 1$  mm; repetition time [TR]/echo time [TE], 8.1/3.7 milliseconds [ms]).

### Image processing

Voxel-Based Morphometry (VBM) and Surface-Based Morphometry (SBM): Volumetric T1 images were segmented into gray matter (GM), white matter (WM), and cerebrospinal fluid (CSF) using the Statistical Parametric Mapping (SPM12) in conjunction with the Computational Anatomy Toolbox (CAT12) [19, 20]. Additionally, surface-based morphometry parameters such as cortical thickness, sulcal depth, and local gyrification index maps were generated. Smoothing was then applied as specified in the original CAT12 pipeline: 15 mm Full width at half maximum (FWHM) Gaussian kernel for cortical thickness, 20 mm for GI and SD, and 25 mm FWHM Gaussian kernel for fractal dimension.

### Segmentation of subcortical and extrapyramidal structures

Bilateral globus pallidus internus and externus (GPi, GPe), habenula, substantia nigra pars compacta and reticulata, and subthalamic nucleus were segmented automatically using a deep learning algorithm DBSegment (<https://github.com/LuxImagingAI/DBSegment>) [16]. Bilateral caudate nucleus, putamen, hippocampus, thalamus, amygdala, and accumbens nucleus were segmented using Synthseg. The estimated total intracranial volume was calculated using SynthSeg (<https://github.com/BBillot/SynthSeg>) [21]. Volumes of the segmented structures were automatically measured, normalized to the total brain volume (TIV), multiplied by 1000, and adjusted structural volume was calculated.

### Statistical analysis

#### Clinical and volumetric data

Statistical analyses were performed using Python 3.9 and libraries such as Scipy, Pandas, Matplotlib, and Seaborn. Participants' demographic information and volumes of segmented subcortical gray matter and extrapyramidal structures were compared using T-Test or Mann Whitney U test, based on their distribution normality using Shapiro-Wilk test. If the data followed a normal distribution, comparisons were made using the T-test; if the data did not follow a normal distribution, the Mann-Whitney U test was used. With 26 subcortical and extrapyramidal structures compared, a Bonferroni correction was applied, setting the significance level at  $p < 1.92 \times 10^{-3}$  (0.05/26).

#### Voxel-based and surface-based morphometry

The voxel-based and surface-based morphometry parameters of the SCA2 and control groups were compared using independent group T-tests. Age was used as a covariate in the General Linear Model (GLM). Additionally, for VBM, total brain volume (TIV) was also used as a covariate. A family-wise error (FWE) corrected alpha value of  $p < 0.05$  was considered statistically significant for comparisons in voxel-based morphometry. For surface-based morphometry parameters, threshold-free cluster enhancement (TFCE) was utilized, and an FWE corrected alpha threshold of 0.05 was considered significant.

## Results

### Demographic data

The patient group had an average age of  $48.71 \pm 13.09$ ; the control group was  $49.83 \pm 19.00$  years old, with no statistically significant difference ( $p=0.877$ ). The control group consisted of 9 males and 7 females, while the patient group included 6 males and 3 females, with no statistically significant difference found in the chi-square test ( $p=0.93$ ).

### Voxel-based morphometry

According to the results of voxel-based morphometry (VBM), SCA2 patients exhibited widespread gray and white matter volume loss in the cerebellum ( $p<0.001$  FWE, Cluster size: 25,918). Additionally, VBM results demonstrated volume reduction in the white matter of pyramidal tracts and cerebellar peduncles within the brainstem formations ( $p<0.001$  FWE, Cluster size: 24557) (Figure 1). No volume changes in gray and white matter were detected in the supratentorial regions.

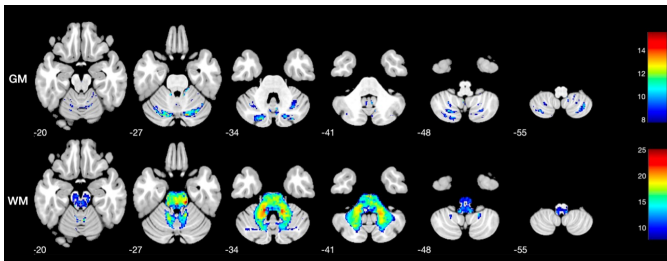


**Figure 1.** Voxel-based morphometry results, GM: Gray Matter, WM: White Matter The bars on the right represent the T value. As the color progresses from blue to red, the T value and statistical significance increase.

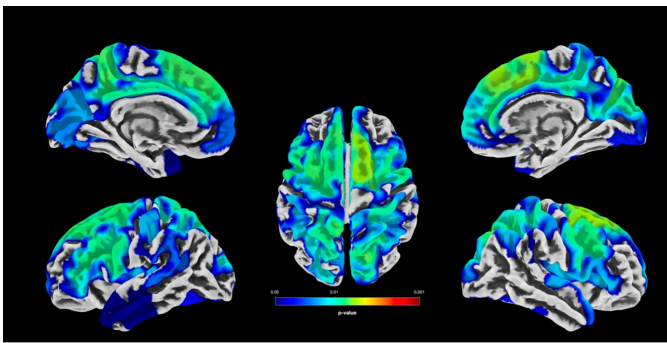


**Figure 2.** Areas showing cortical thickness reduction in SCA2 group ( $p<0.05$  FWE). The bar at the bottom represents the p-value. As the color progresses from blue to red, statistical significance increases, while the p-value decreases.

### Surface-based morphometry

The SCA2 group showed widespread reductions in cortical thickness supratentorially, with these reductions being particularly pronounced in bilateral frontoparietal cortical areas ( $p=0.007$  FWE for right and left hemisphere, Cluster size: 19,276 vertices for left hemisphere; 17,276 vertices

for right hemisphere) (Figure 2, Table 1). Local gyrification index (minimum  $p=0.728$ ), sulcal depth (minimum  $p=0.728$ ), and fractal dimension (minimum  $p=0.676$ ) did not show significant differences between the groups.

**Table 1.** Cortical thickness differences between SCA2 patients and healthy controls.

Cluster index	Labels <sup>a</sup>	Cluster size	x, y, z (mm) <sup>b</sup>
1	L superior frontal 13% L superior parietal 10% L precentral 9% L postcentral 7% L precuneus 7% L supramarginal 6% L inferior parietal 4% L rostral middle frontal 4% L caudal middle frontal 4% Others <sup>c</sup> %36	19.276	16, -75, 45
	R superior frontal 13% R superior parietal 11% R precentral 8% R precuneus 8% R inferior parietal 5% R superior temporal 4% R caudal middle frontal 4% R insula 4% R supramarginal 4% Others <sup>d</sup> 39%	17.276	-6, -47, 48

<sup>a</sup> Labels according to a Desikan Killiany atlas in CAT12. The adjacent percentiles indicate the proportion of vertices in each cluster that are part of that specific region (R: Right, L: Left).

<sup>b</sup> According to the MNI coordinate system.

<sup>c</sup> Others: Parcels that comprise less than 4% of the cluster (posterior cingulate, pars opercularis, insula, lingual, pars triangularis, superior temporal, paracentral, lateral occipital pericalcarine, cuneus, fusiform, isthmus cingulate, caudal anterior cingulate).

<sup>d</sup> Others: Parcels that comprise less than 4% of the cluster (paracentral, pars opercularis, lateral occipital, posterior cingulate, pars triangularis, rostral middle frontal, lingual cuneus, isthmus cingulate, pericalcarine, medial orbitofrontal, fusiform, caudal anterior cingulate, rostral anterior cingulate).

### Volumes of subcortical nuclei and extrapyramidal structures

No statistically significant differences were found in the volumes of subcortical gray matter structures (Left thalamus,  $p=0.729$ ; left caudate,  $p=0.097$ ; left putamen,  $p=0.699$ ; left hippocampus,  $p=0.416$ ; Left accumbens area,  $p=0.322$ ; right thalamus,  $p=0.205$ ; right caudate,  $p=0.183$ ; right putamen,  $p=0.236$ ; right hippocampus,  $p=0.645$ ; right accumbens area,  $p=0.630$ ) between the patients and the control group. When comparing the volumes of extrapyramidal structures, it was found that the volume of the left red nucleus was calculated to be  $0.13 \pm 0.01$  ml in healthy controls and  $0.11 \pm 0.01$  ml in SCA2 patients, showing a decrease in the patient group ( $p=0.019$ ).

**Table 2.** Volumes of subcortical gray matter and extrapyramidal structures.

TIV Corrected Structure Volume	Healthy Control (n=16)	SCA2 (n=9)	p value
Left thalamus	4.28 ± 0.40 (4.07-4.49)	4.23 ± 0.34 (3.97-4.49)	0.729
Left caudate	2.42 ± 0.28 (2.27-2.57)	2.23 ± 0.25 (2.04-2.42)	0.097
Left putamen	3.41 ± 0.30 (3.25-3.57)	3.36 ± 0.31 (3.13-3.60)	0.699
Left hippocampus	2.76 ± 0.24 (2.63-2.89)	2.67 ± 0.28 (2.45-2.89)	0.416
Left amygdala	1.11 (IQR: 0.10) (1.04-1.14)	1.03 (IQR: 0.05) (0.96-1.10)	0.075*
Left accumbens area	0.42 ± 0.05 (0.39-0.45)	0.40 ± 0.05 (0.36-0.43)	0.322
Right thalamus	4.32 ± 0.36 (4.13-4.52)	4.14 ± 0.32 (3.89-4.39)	0.205
Right caudate	2.50 (IQR: 0.27) (2.33-2.58)	2.18 (IQR: 0.44) (2.16-2.65)	0.183*
Right putamen	3.35 ± 0.27 (3.20-3.49)	3.22 ± 0.23 (3.04-3.40)	0.236
Right hippocampus	2.72 ± 0.23 (2.60-2.84)	2.67 ± 0.25 (2.48-2.87)	0.645
Right amygdala	1.07 ± 0.08 (1.03-1.12)	1.10 ± 0.08 (1.04-1.16)	0.507
Right accumbens area	0.39 ± 0.05 (0.37-0.42)	0.38 ± 0.06 (0.33-0.43)	0.630
Left globus pallidus externus	0.45 ± 0.04 (0.43-0.47)	0.44 ± 0.03 (0.42-0.46)	0.620
Right globus pallidus externus	0.42 ± 0.04 (0.40-0.44)	0.42 ± 0.03 (0.40-0.44)	0.891
Left globus pallidus internus	0.21 ± 0.02 (0.20-0.22)	0.21 ± 0.01 (0.19-0.22)	0.849
Right globus pallidus internus	0.21 ± 0.02 (0.20-0.22)	0.20 ± 0.02 (0.19-0.21)	0.322
Left habenula	0.02 ± 0.00 (0.02-0.02)	0.02 ± 0.00 (0.02-0.02)	0.461
Right habenula	0.01 ± 0.00 (0.01-0.02)	0.02 ± 0.00 (0.01-0.02)	0.314
Left red nucleus	0.13 ± 0.01 (0.12-0.13)	0.11 ± 0.01 (0.10-0.12)	0.019
Right red nucleus	0.12 ± 0.01 (0.11-0.12)	0.10 ± 0.01 (0.10-0.11)	0.001
Left substansia nigra pars compacta	0.05 ± 0.00 (0.04-0.05)	0.04 ± 0.00 (0.03-0.04)	<0.001
Right substansia nigra pars compacta	0.04 ± 0.00 (0.04-0.05)	0.03 ± 0.01 (0.03-0.04)	0.001
Left substansia nigra pars reticularis	0.06 ± 0.01 (0.06-0.07)	0.06 ± 0.01 (0.05-0.06)	<0.001
Right substansia nigra pars reticularis	0.07 ± 0.01 (0.06-0.07)	0.06 ± 0.00 (0.05-0.06)	<0.001
Left subthalamic nucleus	0.10 ± 0.01 (0.10-0.10)	0.08 ± 0.01 (0.07-0.09)	0.015
Right subthalamic nucleus	0.10 ± 0.01 (0.10-0.10)	0.08 ± 0.01 (0.07-0.09)	0.001

\* Rows marked with \* indicate that the data did not follow a normal distribution according to the Shapiro-Wilk test, so the Mann-Whitney U test was applied. For data that followed a normal distribution, the T-test was applied. In these rows, unlike the others, the data are presented as median (IQR) instead of mean ± standard deviation. The values in parentheses represent the 95% confidence intervals for the data in that group. TIV: Total intracranial volume, SCA2: Spinocerebellar ataxia type 2.

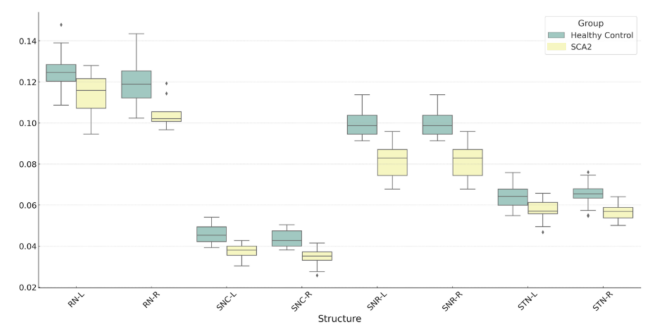


**Figure 3.** Box-plot representation of volumetric findings in extrapyramidal structures.

The volume of the right red nucleus was calculated to be  $0.12 \pm 0.01$  ml in healthy controls and  $0.1 \pm 0.01$  ml in SCA2 patients, also showing a decrease in the patient group ( $p=0.001$ ). The volume of the left substantia nigra pars compacta was calculated to be  $0.05 \pm 0.003$  ml in healthy controls and  $0.04 \pm 0.001$  ml in SCA2 patients, indicating a decrease in the patient group ( $p<0.001$ ). The volume of the right substantia nigra pars compacta was calculated to be  $0.04 \pm 0.002$  ml in healthy controls and  $0.03 \pm 0.001$  ml in SCA2 patients, indicating a decrease in the patient group ( $p=0.001$ ). The volume of the left substantia nigra pars reticulata was calculated to be  $0.05 \pm 0.003$  ml in healthy controls and  $0.04 \pm 0.001$  ml in SCA2 patients, showing a decrease in the patient group ( $p<0.001$ ). The volume of the right substantia nigra pars reticulata was calculated to be  $0.04 \pm 0.002$  ml in healthy controls and  $0.03 \pm 0.01$  ml in SCA2 patients, indicating a decrease in the patient group ( $p<0.001$ ). The volume of the right subthalamic nucleus was calculated to be  $0.07 \pm 0.01$  ml in healthy controls and  $0.06 \pm 0.004$  ml in SCA2 patients, showing a statistically significant decrease in the patient group ( $p=0.001$ ) (Table 2, Figure 3).

**Discussion**

In this study, a comprehensive volumetric perspective was applied to examine cortical morphological changes in SCA2 patients by investigating the volumes of gray and white matter areas as well as subcortical and extrapyramidal structures. VBM findings, as expected, revealed widespread cerebellar gray matter volume loss and white matter loss in the brainstem in SCA2 patients. However, no gray matter loss was detected in supratentorial structures. SBM identified widespread cortical thickness reduction in supratentorial areas, especially in the frontoparietal lobes. Furthermore, this study is the first to our knowledge to radiologically demonstrate volume loss in the subthalamic nucleus, red nuclei, and both the pars compacta and reticulata of the substantia nigra. No significant volume difference was shown in subcortical gray matter structures. These studies, similar to other studies in the literature, demonstrate both infratentorial and supratentorial involvement, as well as extrapyramidal involvement in SCA2 patients [22].

To date, both cross-sectional and longitudinal VBM studies conducted on SCA2 patients have demonstrated atrophy in the cerebellum and brainstem, which is consistent

with this study findings [4, 9, 23, 24, 25]. The findings in the supratentorial area from VBM studies are contradictory, with only a limited number of studies, differing from this study, showing gray matter volume loss in the parahippocampal gyrus. One such study that found atrophy in the parahippocampal gyrus used an uncorrected statistical threshold of  $p < 0.005$ , which can lead to false positives in VBM studies [8]. This study employed a family-wise error correction to avoid false positives, which might explain the differences in study outcomes.

VBM findings for white matter indicate widespread volume reduction in infratentorial white matter structures in SCA2 patients. However, we did not detect any volume reduction in supratentorial white matter. This is intriguing, as two studies using the DTI component of this dataset have shown a decrease in fiber density (FD), fiber cross-section (FC), and fiber density and cross-section (FDC) in supratentorial white matter structures in SCA2 patients. In another DTI study conducted with this dataset [26], Tract-Based Spatial Statistics (TBSS) was used to examine fractional anisotropy (FA), mean diffusivity (MD), radial diffusivity (RD), and axial diffusivity (AD) values in white matter tracts. This study revealed widespread FA reduction and RD increase in infratentorial white matter tracts, as well as a limited FA reduction in white matter tracts associated with the corticospinal tract [27]. Although macroscopic infratentorial structural changes could be detected in this study, no supratentorial macroscopic structural changes were observed. This may be related to the superiority of diffusion tensor imaging (DTI) in detecting microstructural changes.

Surface-based morphometry studies in SCA2 patients are relatively rare. A study by Nigri and colleagues investigated SCA2 patients in the early preclinical stage and found supratentorial cortical thickness reduction, more pronounced in the frontal areas, even at this stage, with longitudinal analysis showing that the reduction in cortical thickness became more apparent over time [11]. PET studies have shown decreased cortical FDG uptake [28, 29, 30], and MR-Spectroscopy studies have found decreased N-acetyl aspartate/Choline ratios in the frontal cortex of SCA2 patients [31], consistent with a reduction in neuronal load. fMRI studies have detected decreased functional connectivity between the cerebellum and cortex [32, 33]. This study is the first to demonstrate widespread and pronounced cortical thinning in symptomatic SCA2 patients, and these findings are consistent with the widespread cortical involvement shown in other studies.

This study is the first to radiologically reveal volume loss in the substantia nigra, subthalamic nucleus, and red nucleus in SCA2 patients. In the postmortem study conducted by Schöls and colleagues, patients with SCA2 similarly showed a loss of volume in the subthalamic nucleus and globus pallidus, akin to this study. Rüb and colleagues, in autopsy studies related to SCA2 patients, have similarly demonstrated volume loss in the red nucleus histologically, aligning with these study findings. Combined with autopsy studies from the literature, this study results could explain the extrapyramidal involvement observed in patients.

This study has several limitations. Firstly, study findings

could not be validated with neurocognitive tests due to their absence. Additionally, only a limited number of patients could be included in the study. Further studies with larger patient series and clinical findings such as neurocognitive tests could support these study findings.

## Conclusion

In conclusion, SCA2 patients not only exhibit widespread gray matter loss in the cerebellum but also white matter volume loss in the brainstem. These patients have more pronounced widespread cortical thinning in the frontoparietal areas. Moreover, this study demonstrated widespread volume loss in the substantia nigra, subthalamic nucleus, and red nuclei, suggesting extrapyramidal involvement. Future comprehensive studies incorporating a larger number of patients and clinical findings, such as neurocognitive tests, could reinforce these study findings.

## Ethical approval

Ethical approval was obtained for this study from the Ondokuz Mayıs University Clinical Research Ethics Committee (Decision no: 2024/171).

## References

1. L. Velázquez-Pérez et al., "Neurophysiological features in spinocerebellar ataxia type 2: Prospects for novel biomarkers," *Clinical Neurophysiology*, vol. 135, pp. 1–12, 2022, doi: <https://doi.org/10.1016/j.clinph.2021.12.005>.
2. G. W. J. Auburger, "Chapter 26 - Spinocerebellar ataxia type 2," in *Handbook of Clinical Neurology*, vol. 103, S. H. Subramony and A. Dürr, Eds., Elsevier, 2012, pp. 423–436. doi: <https://doi.org/10.1016/B978-0-444-51892-7.00026-7>.
3. L. C. Velázquez-Pérez et al., "Spinocerebellar ataxia type 2: Clinicogenetic aspects, mechanistic insights, and management approaches," Sep. 11, 2017, *Frontiers Media S.A.* doi: 10.3389/fneur.2017.00472.
4. G. Goel et al., "Gray matter volume deficits in spinocerebellar ataxia: An optimized voxel based morphometric study," *Parkinsonism Relat Disord*, vol. 17, no. 7, pp. 521–527, Aug. 2011, doi: 10.1016/j.parkreldis.2011.04.008.
5. R. Della Nave et al., "Brain white matter damage in SCA1 and SCA2. An in vivo study using voxel-based morphometry, histogram analysis of mean diffusivity and tract-based spatial statistics," *Neuroimage*, vol. 43, no. 1, pp. 10–19, 2008, doi: <https://doi.org/10.1016/j.neuroimage.2008.06.036>.
6. C. Brenneis et al., "Atrophy pattern in SCA2 determined by voxel-based morphometry," *Neuroreport*, vol. 14, no. 14, 2003, [Online]. Available: [https://journals.lww.com/neuroreport/fulltext/2003/10060/atrophy\\_pattern\\_in\\_sca2\\_determined\\_by\\_voxel\\_based.8.aspx](https://journals.lww.com/neuroreport/fulltext/2003/10060/atrophy_pattern_in_sca2_determined_by_voxel_based.8.aspx).
7. R. Della Nave et al., "Brain structural damage in spinocerebellar ataxia type 2. A voxel-based morphometry study," *Movement Disorders*, vol. 23, no. 6, pp. 899–903, Apr. 2008, doi: 10.1002/mds.21982.
8. R. E. Mercadillo et al., "Parahippocampal gray matter alterations in Spinocerebellar Ataxia Type 2 identified by voxel based morphometry," *J Neurol Sci*, vol. 347, no. 1–2, pp. 50–58, Dec. 2014, doi: 10.1016/j.jns.2014.09.018.
9. Q. Han et al., "Voxel-based meta-analysis of gray and white matter volume abnormalities in spinocerebellar ataxia type 2," *Brain Behav*, vol. 8, no. 9, Sep. 2018, doi: 10.1002/brb3.1099.
10. M. Goto et al., "Advantages of Using Both Voxel-and Surface-based Morphometry in Cortical Morphology Analysis: A Review of Various Applications," 2022, *Japanese Society for Magnetic Resonance in Medicine*. doi: 10.2463/mrms.rev.2021-0096.
11. A. Nigri et al., "Progression of Cerebellar Atrophy in Spinocerebellar Ataxia Type 2 Gene Carriers: A Longitudinal MRI Study in Preclinical and Early Disease Stages," *Front Neurol*, vol. 11, Dec. 2020, doi: 10.3389/fneur.2020.616419.

12. C. Marzi et al., “Structural Complexity of the Cerebellum and Cerebral Cortex is Reduced in Spinocerebellar Ataxia Type 2,” *Journal of Neuroimaging*, vol. 28, no. 6, pp. 688–693, Nov. 2018, doi: 10.1111/jon.12534.
13. K. Cai et al., “Identification of early-stage Alzheimer’s disease using sulcal morphology and other common neuroimaging indices,” *PLoS One*, vol. 12, no. 1, Jan. 2017, doi: 10.1371/journal.pone.0170875.
14. M. Li et al., “Cortical morphology of chronic users of codeine-containing cough syrups: association with sulcal depth, gyrification, and cortical thickness,” *Eur Radiol*, vol. 29, no. 11, pp. 5901–5909, Nov. 2019, doi: 10.1007/s00330-019-06165-0.
15. L. Schöls et al., “No parkinsonism in SCA2 and SCA3 despite severe neurodegeneration of the dopaminergic substantia nigra,” 2024, doi: 10.1093/awv253.
16. M. Baniasadi et al., “DBSegment: Fast and robust segmentation of deep brain structures considering domain generalization,” *Hum Brain Mapp*, vol. 44, no. 2, pp. 762–778, Feb. 2023, doi: 10.1002/hbm.26097.
17. M. Mascalchi et al., “Histogram analysis of dti-derived indices reveals pontocerebellar degeneration and its progression in SCA2,” *PLoS One*, vol. 13, no. 7, Jul. 2018, doi: 10.1371/journal.pone.0200258.
18. S. Cuschieri, “The STROBE guidelines,” Apr. 01, 2019, Wolters Kluwer Medknow Publications. doi: 10.4103/sja.SJA\_543\_18.
19. J. Ashburner and K. J. Friston, “Unified segmentation,” *Neuroimage*, vol. 26, no. 3, pp. 839–851, 2005, doi: <https://doi.org/10.1016/j.neuroimage.2005.02.018>.
20. C. Gaser et al., “CAT: a computational anatomy toolbox for the analysis of structural MRI data,” *Gigascience*, vol. 13, p. giae049, Jan. 2024, doi: 10.1093/gigascience/giae049.
21. B. Billot et al., “SynthSeg: Segmentation of brain MRI scans of any contrast and resolution without retraining,” *Med Image Anal*, vol. 86, May 2023, doi: 10.1016/j.media.2023.102789.
22. M. Mascalchi and A. Vella, “Neuroimaging biomarkers in SCA2 gene carriers,” Feb. 01, 2020, MDPI AG. doi: 10.3390/ijms21031020.
23. Q. Han et al., “Voxel-based meta-analysis of gray and white matter volume abnormalities in spinocerebellar ataxia type 2,” *Brain Behav*, vol. 8, no. 9, Sep. 2018, doi: 10.1002/brb3.1099.
24. Q. Han et al., “Voxel-based meta-analysis of gray and white matter volume abnormalities in spinocerebellar ataxia type 2,” *Brain Behav*, vol. 8, no. 9, Sep. 2018, doi: 10.1002/brb3.1099.
25. R. Della Nave et al., “Brain structural damage in spinocerebellar ataxia type 2. A voxel-based morphometry study,” *Movement Disorders*, vol. 23, no. 6, pp. 899–903, Apr. 2008, doi: 10.1002/mds.21982.
26. Y. Tu et al., “Progressive white matter degeneration in patients with spinocerebellar ataxia type 2,” *Neuroradiology*, vol. 66, no. 1, pp. 101–108, Jan. 2024, doi: 10.1007/s00234-023-03260-4.
27. N. Al-Arab and S. Hannoun, “White matter integrity assessment in spinocerebellar ataxia type 2 (SCA2) patients,” *Clin Radiol*, vol. 79, no. 1, pp. 67–72, Jan. 2024, doi: 10.1016/j.crad.2023.10.020.
28. M. Oh et al., “Different subregional metabolism patterns in patients with cerebellar ataxia by 18Ffluorodeoxyglucose positron emission tomography,” *PLoS One*, vol. 12, no. 3, Mar. 2017, doi: 10.1371/journal.pone.0173275.
29. P. S. Wang et al., “Regional patterns of cerebral glucose metabolism in spinocerebellar ataxia type 2, 3 and 6: A voxel-based FDG-positron emission tomography analysis,” *J Neurol*, vol. 254, no. 7, pp. 838–845, Jul. 2007, doi: 10.1007/s00415-006-0383-9.
30. A. Inagaki et al., “Positron emission tomography and magnetic resonance imaging in spinocerebellar ataxia type 2: A study of symptomatic and asymptomatic individuals,” *Eur J Neurol*, vol. 12, no. 9, pp. 725–728, Sep. 2005, doi: 10.1111/j.1468-1331.2005.01011.x.
31. M. Viau et al., “1H magnetic resonance spectroscopy of autosomal ataxias,” *Brain Res*, vol. 1049, no. 2, pp. 191–202, 2005, doi: <https://doi.org/10.1016/j.brainres.2005.05.015>.
32. G. Olivito et al., “Neural substrates of motor and cognitive dysfunctions in SCA2 patients: A network based statistics analysis,” *Neuroimage Clin*, vol. 14, pp. 719–725, 2017, doi: <https://doi.org/10.1016/j.nicl.2017.03.009>.
33. C. R. Hernandez-Castillo et al., “Functional connectivity changes related to cognitive and motor performance in spinocerebellar ataxia type 2,” *Movement Disorders*, vol. 30, no. 10, pp. 1391–1399, Sep. 2015, doi: <https://doi.org/10.1002/mds.26320>.